IRAMP
5(1), June 2014, pp. 61-71

© International Science Press
ISSN: 2229-3159

Spectral Line Shapes Strongly Affected by Magnetic-Field-Caused Modifications of Trajectories of Plasma Electrons

E. OKS

Physics Department, 206 Allison Lab., Auburn University, Auburn, AL 36849, USA

ABSTRACT: We develop the general framework for calculating shapes of hydrogen (or deuterium) spectral lines in strongly-magnetized plasmas allowing for spiraling trajectories of perturbing electrons. We show that in this situation the first order term $\Phi^{(1)}(B)$ of the Dyson expansion of the electron broadening operator does not vanish – in distinction to the case of rectilinear trajectories, where the first non-vanishing term appeared only in the second order. We use as an example the Ly_α line to illustrate the effects of the spiraling trajectories. We show that the shape of *each* of the two σ-components can become a doublet: in addition to the shifted component, there can appear also an unshifted component. Moreover, the shape of *each* of the two σ-components can also become a triplet: in addition to the shifted and unshifted component, there can appear also a component shifted to the opposite wing of the line. Both the positions and the intensities of the shifted components depend strongly on the magnitude of $\Phi^{(1)}(B)$.

PACS numbers: 32.70.JZ, 52.25.Xz, 32.60.+i, 52.55.Fa

1. INTRODUCTION

All semiclassical theories of the Stark broadening of spectral lines in plasmas by electrons considered either rectilinear trajectories of plasma electrons in the case of neutral radiating atoms (hereafter, radiators) or hyperbolic trajectories in the case of charged radiators – see, *e.g.*, books [1, 2]. However, in many types of plasmas – such as, *e.g.*, tokamak plasmas (see, *e.g.*, [3]), laser-produced plasmas (see, *e.g.*, [4]), capacitor-produced plasmas [5] – there are strong magnetic fields. In a strong magnetic field *B*, perturbing electrons basically spiral along magnetic field lines. Therefore, their trajectories are not rectilinear in the case of neutral radiators or not hyperbolic in the case of charged radiators.

In the present paper we take this into account. First, we develop the general framework for calculating shapes of hydrogen (or deuterium) spectral lines in strongly-magnetized plasmas allowing for spiraling trajectories of perturbing electrons. We show that in this situation the first order term $\Phi^{(1)}$(B) of the Dyson expansion of the electron broadening operator does not vanish – in distinction to the case of rectilinear trajectories, where the first non-vanishing term appeared only in the second order. Another situation, where $\Phi^{(1)}$ was non-zero, had been previously presented in our works [6, 7], where instead of the magnetic field, we took into account a strong laser field: it caused an oscillatory motion of perturbing electrons and resulted in a shift of the entire spectral line (called electron oscillatory shift).

Then we calculate the shapes of the Ly_α line. We show that, while the shape of the π-component remains the same as for rectilinear trajectories, the shape of the σ-components is strongly affected by the allowance for the spiraling trajectories. Namely, the shape of *each* of the two σ-component can become a doublet: in addition to the shifted component, there can appear also an unshifted component. Moreover, the shape of *each* of the two σ-components can also become a triplet: in addition to the shifted and unshifted component, there can appear also a component shifted to the opposite wing of the line. Both the positions and the intensities of the shifted components depend strongly on the magnitude of $\Phi^{(1)}(B)$.

2. THE GENERAL FRAMEWORK

We consider a plasma containing a strong magnetic field **B**. We choose the z-axis along **B**. For the case of neutral radiators, the radius-vector of a perturbing electron can be represented in the form

$$\mathbf{R}(t) = \rho\mathbf{e}_x + v_z t\mathbf{e}_z + r_{Bp}\,[\mathbf{e}_x \cos(\omega_B t + \varphi) + \mathbf{e}_y \sin(\omega_B t + \varphi)], \tag{1}$$

where the x-axis is chosen along the impact parameter vector $\boldsymbol{\rho}$. Here v_z is the electron velocity along the magnetic field and

$$r_{Bp} = v_p/\omega_B,\ \omega_B = eB/(m_e c), \tag{2}$$

where v_p is the electron velocity in the plane perpendicular to **B**; ω_B is the Larmor frequency.

For the atomic electron to experience the spiraling nature of the trajectories of perturbing electrons, it requires $\rho_{De}/r_{Bp} > 1$, where ρ_{De} is the electron Debye radius. Taking into account that the average over the 2D-Maxwell distribution $<1/v_p> = \pi^{1/2}/v_{Te}$, where $v_{Te} = (2T_e/m_e)^{1/2}$ is the mean thermal velocity of perturbing electrons, the condition $\rho_{De}/r_{Bp} > 1$ can be rewritten in the form $\pi^{1/2}\omega_B/\omega_{pe} > 1$ (where ω_{pe} is the plasma electron frequency) or

$$B > B_{cr} = (4N_e a_B)^{1/2},\ B_{cr}(\text{Tesla}) = 1.81 \times 10^{-7}[N_e(\text{cm}^{-3})]^{1/2} \tag{3}$$

(a_B is the Bohr radius). For example, for the edge plasmas in tokamaks, at $N_e = 10^{14}$ cm^{-3}, the condition (3) becomes $B > 1.8$ Tesla, which is fulfilled in modern tokamaks. The condition (3) is easily fulfilled in capacitor-produced plasmas [5] and in plasmas produced by high-intensity lasers [4] (in the latter case, radiators would be charged rather than neutral).

We consider the situation where the temperature T of the radiators satisfies the condition

$$T << (11.12\ keV/n)(M/M_H)^2, \tag{4}$$

where M is the radiator mass, M_H is the mass of hydrogen atoms, n is the principal quantum number of the energy levels, from which the spectral line originates. Under this condition, the Lorentz field effects can be disregarded compared to the "pure" magnetic field effects.

To get the message across in a relatively simple form, we limit ourselves by the Lyman lines. Then matrix elements of the electron broadening operator in the impact approximation have the form

$$\Phi_{\alpha\alpha'} = N_e \int_0^\infty dv_p W_p(v_p) \int_{-\infty}^\infty dv_z W_z(v_z) v_z \int_0^{\rho\max} 2\pi\rho < S_{\alpha\alpha'} - 1 >, \tag{5}$$

where N_e is the electron density, $W_p(v_p)$ is the 2D-Maxwell distribution of the perpendicular velocities, $W_z(v_z)$ is the 1D-Maxwell (Boltzmann) distribution of the longitudinal velocities, $\rho\max = \rho_{De}$ is the maximum impact parameter, S is the scattering matrix, <...> stands for averaging; α and α' label sublevels of the upper energy level involved in the radiative transition.

In the first order of the Dyson expansion we have

$$S_{\alpha\alpha'} - 1 = -i(e^2/\hbar)\int_0^\infty dt\{\mathbf{r}_{\alpha\alpha'}\mathbf{R}(t)/[R(t)]^3\}\exp(i\omega_{\alpha\alpha'}\, t), \tag{6}$$

where **r** is the radius-vector of the atomic electron, $\mathbf{r}_{\alpha\alpha'}\,\mathbf{R}$ is the scalar product (also known as the dot-product). Here $\omega_{\alpha\alpha'}$ is the energy difference between the energy sublevels α and α' divided by $\hbar$ for the adjacent energy sublevels we have

$$|\omega_{\alpha\alpha'}| = \omega_B/2. \tag{7}$$

We introduce the following notations:

$$s = \rho/r_{Bp},\ g = v_z/v_p,\ w = v_z t/r_{Bp} \tag{8}$$

In these notations, Eq. (6) can be rewritten as

$$S_{\alpha\alpha'} - 1 = -i(e^2/(\hbar r_{Bp} v_z)\int_{-\infty}^{\infty} dw$$

$$\{z_{\alpha\alpha'} w\delta_{\alpha\alpha'} + \exp[\pm iw/(2g)]\,[y_{\alpha\alpha'}\sin(w/g+\varphi) + x_{\alpha\alpha'}(\cos(w/g+\varphi)+s)]\}/[1 + w^2 + 2s\cos(w/g+\varphi) + s^2]^{3/2}, \tag{9}$$

where $\delta_{\alpha\alpha'}$ is the Kronecker-delta (we use the parabolic quantization).

In the integrand in eq. (9), the terms containing $z_{\alpha\alpha'}$ is the odd function of w, so that the corresponding integral vanishes. The term containing $y_{\alpha\alpha'}$ vanishes after averaging over the phase φ. As for the term containing $x_{\alpha\alpha'}$ after averaging over the phase φ, it becomes as follows (it should be noted that in this setup the angular averaging of vector ρ is irrelevant – in distinction to the rectilinear trajectories)

$$< S_{\alpha\alpha'} - 1 > = -i[e^2/(\hbar r_{Bp} v_z)]\int_{-\infty}^{\infty} dw\cos[w/(2g)]\ \{\mathbf{K}[4s/j(w,s)] - \mathbf{E}[4s/j(w,s)](w^2 + 1 - s^2)/[w^2 + (s-1)^2]\}/\{\pi s[j(w,s)]^{1/2}\} \tag{10}$$

where $\mathbf{K}(u)$ and $\mathbf{E}(u)$ are the elliptic integrals, and

$$j(w, s) = w^2 + (1 + s)^2. \tag{11}$$

We denote

$$u = \rho_{De}/r_{Bp} \tag{12}$$

Then, combining eqs. (5) and (10), the first order of the *nondiagonal* elements of the electron broadening operator $\Phi_{\alpha\alpha'}{}^{(1)}$ can be represented in the form (the diagonal elements of $\Phi^{(1)}$ vanish because the diagonal elements of the x-coordinate are zeros):

$$\Phi_{\alpha\alpha'}{}^{(1)} = -ix_{\alpha\alpha'}(e^2/\hbar)\rho_{De}N_e\int_0^{\infty} dv_p W_p(v_p)\int_{-\infty}^{\infty} dv_z W_z(v_z)\, f_0(g,u) \tag{13}$$

where

$$f_0(g,\ u) = (1/u)\int_0^u ds\int_{-\infty}^{\infty} dw$$

$$\cos[w/(2g)]\{K[4s/j(w,s)] - E[4s/j(w,s)](w^2 + 1 - s^2)/[w^2 + (s-1)^2]\}/\{\pi s[j(w,s)]^{1/2}\} \tag{14}$$

We note that $\Phi_{\alpha\alpha'}{}^{(1)}$ scales with the electron density as $N_e{}^{1/2}$.

For obtaining results in the simplest form, we calculate the average $< g > = < v_z/v_p >$

$$< g > = \int_0^{\infty} dv_p W_p(v_p)\int_{-\infty}^{\infty} dv_z W_z(v_z) v_z/v_p = 1 \tag{15}$$

and denote $f_0(g, u) = f(u)$. The argument can be represented as $u = B/B_{cr}$, where B_{cr} is the critical value of the magnetic field defined in eq. (3). Figure 1 shows this universal function $f(u)$ that controls the phenomenon under consideration.

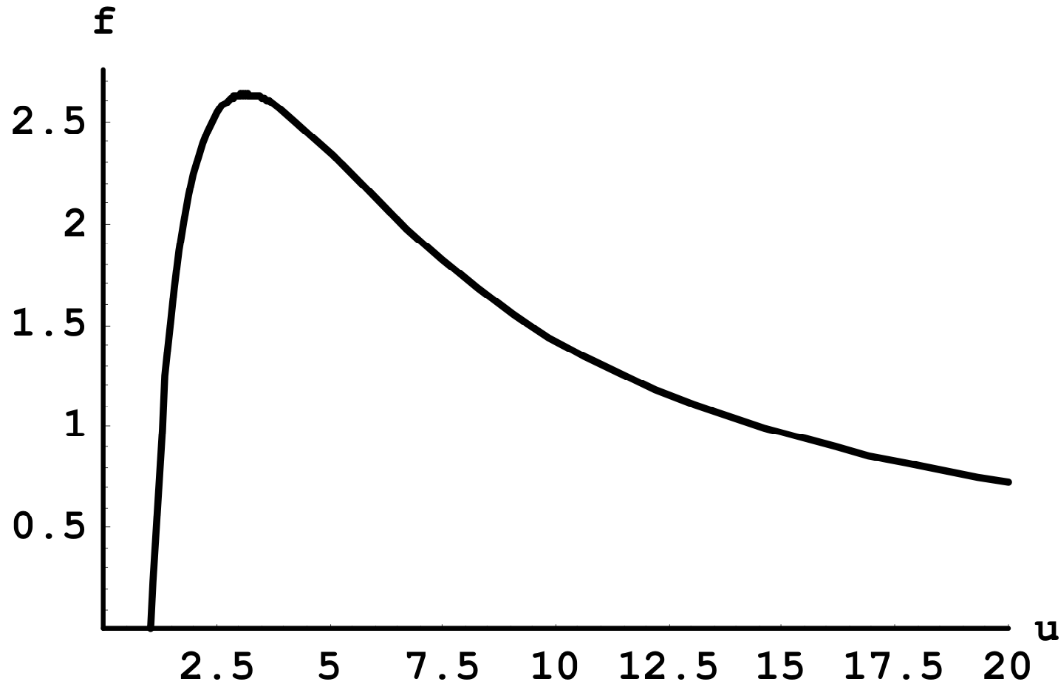

Figure 1: The universal function *f* (*u*) that controls the first order of the electron broadening operator. The argument $u = B/B_{cr}$, where B_{cr} is the critical value of the magnetic field defined in eq. (3).

It is seen that $f(u)$ starts growing at $B/B_{cr} > 1$, reaches the maximum at $B/B_{cr} = 3$, and then gradually diminishes as B/B_{cr} further increases.

The presence of the maximum of $f(u)$ can be physically understood as follows. At $\rho_{De} < r_{Bp}$ the effect is absent because the radius of the spirals of the trajectory of perturbing electrons exceeds the Debye radius. In the opposite limit, *i.e.*, at $\rho_{De} >> r_{Bp}$, the radius of the spirals of the trajectory is so small (compared to the Debye radius), that the atomic electron perceives the trajectory almost as a straight line (the straight line of a "width" ~ r_{Bp}), so that $\Phi_{\alpha\alpha'}^{(1)}$ gradually goes to the limit of zero, *i.e.*, to the limit corresponding to rectilinear trajectories of perturbing electrons.

3. SHAPES OF THE Ly_α LINE

3.1. For calculating the shapes of the Ly_α line we use the parabolic quantization, *i.e.*, the quantum numbers $(n_1 n_2 m)$. We denote the four sublevels of the upper level ($n = 2$) as follows: (001) as 1, (100) as 2, (00-1) as 3, and (010) as 4. According to the linear Zeeman effect, states 1 and 3 are shifted (in the frequency scale) by $\omega_B/2$ and $-\omega_B/2$, respectively, while the states 2 and 4 remain unshifted. The shifts are counted from the unperturbed position of the $n = 2$ energy level.

The nonzero matrix elements of the x-coordinates within the $n = 2$ space are the following:

$$x_{12} = x_{21} = x_{23} = x_{32} = x_{34} = x_{43} = x_{41} = x_{14} = -3a_B/2 \quad (16)$$

We denote

$$a = [3\hbar/(2m_e)]\rho_{De} N_e f[B/B_{cr}],\ d = \omega_B/2 \quad (17)$$

The lineshapes of the Ly-line are controlled by matrix elements of operator G^{-1}, where the operator G is defined as follows

$$G_{\alpha\alpha'} = < \alpha|i[\omega - \Delta_{\alpha\alpha'}(B)] + \Phi]|\alpha' > \tag{18}$$

where $\Delta_{11} = d$, $\Delta_{33} = -d$, $\Delta_{22} = \Delta_{44} = 0$. Here and below, ω is counted from the unperturbed frequency of the spectral line. In order to present in the purest form how the nonvanishing first order of the electron broadening operator $Ö^{(1)}$ affects the lineshapes, we consider two situations where there is no need to include the effect of the spiraling trajectories of perturbing electron on $\Phi^{(2)}$.

3.2. The first situation is where there is a sufficiently strong Langmuir turbulence in a plasma. In this situation, by extending the results from [8, 9] to a strong Langmuir turbulence, we find that the real part of all diagonal elements of the operator G is practically equal to γ_p, which is the largest of the characteristic frequencies of various nonlinear processes involving Langmuir turbulence in the plasma – the processes such as, *e.g.*, the generation of Langmuir turbulence, the induced scattering on the charged particles, the nonlinear decay into ionic sound, and so on (the frequency γ_p is assumed to control the width of the power spectrum of Langmuir turbulence). Then matrix G takes the form (we omitted the suffix "p" of γ_p).

$$G = \begin{vmatrix} i(\omega - d) + \gamma & ia & 0 & ia \\ ia & i\omega + \gamma & ia & 0 \\ 0 & ia & i\omega + \gamma & ia \\ ia & 0 & ia & i(\omega + d + \gamma) \end{vmatrix} \tag{19}$$

The general expression for the lineshape $I(\omega)$ of Ly-lines is

$$I(\omega) = \text{const Re}\left[\sum_{\alpha\alpha'} \mathbf{r}_{a0} {}^* \mathbf{r}_{\alpha'0} < \alpha\left|G^{-1}\right|\alpha' >\right] \tag{20}$$

where suffix "0" denotes the ground state. For the Ly_α line, the nonzero matrix elements of the operator r in eq. (20) are as follows (see, *e.g.*, [10]):

$$< 4|x|0 > = < 2|x|0 > = < 3|z|0 > = -< 1|z|0 > = 128a_B/243, \quad < 4|y|0 > = -< 2|y|0 > = 128ia_B/243. \tag{21}$$

After inverting the matrix G we obtain the following normalized profiles for each component of the Ly_α line. For the π-component:

$$I(\omega) = (\gamma/\pi)/(\gamma^2 + \omega^2) \tag{21}$$

For the σ-component originating from state (001):

$$I(\omega) = (\gamma/\pi)[\omega^4 + 2d\omega^3 + (d^2 - 2a^2 + 2\gamma^2)\,\omega^2 + 2d\gamma^2\omega + 8a^4 + 2a^2d^2 + \gamma^2d^2 + 6\gamma^2a^2 + \gamma^4]/\{(\gamma^2 + \omega^2)$$
$$[\omega^4 - 2(d^2 + 4a^2 - \gamma^2)\omega^2 + (d^2 + 4a^2 + \gamma^2)^2]\}. \tag{22}$$

For the σ-component originating from state (00–1), the normalized profile can be obtained from eq. (22) by changing d to $-d$.

It is seen that, while the profile of the π-component remains unaffected by the allowance for the spiraling trajectories of perturbing electrons, the profiles of the σ-components are significantly affected by the allowance for the spiraling trajectories of perturbing electrons – both qualitatively and quantitatively: *each* of the two ó-components could generally become a triplet. Indeed, the first factor in denominator in eq. (22), *i.e.*, the factor $(\gamma^2 + \omega^2)$ has the minimum at $\omega = 0$. This translates into the appearance of the unshifted σ-subcomponent (*i.e.*, the component peaked at $\omega = 0$.

The second factor in denominator in eq. (22) has the minima at $\omega = \pm(d^2 + 4a^2 - \gamma^2)^{1/2}$. This translates into two additional new features. For example, for the σ-component originating from state (001), first, the position of the subcomponent shifted to the blue side changes from d to $(d^2 + 4a^2 - \gamma^2)^{1/2}$. At relatively small γ, the new position of this subcomponent is approximately $(d^2 + 4a^2)^{1/2}$, where d linearly depends on the magnetic field B (according to eqs. (2), (17)), while a depends on B in a more complicated way: $a(B)$ is proportional to the function $f\,[B/B_{cr}]$, whose plot was presented in Fig. 1. Second, in addition to the blue-shifted and unshifted component, there can appear also a component shifted to the opposite (red) wing of the line. This illustrated in Fig. 2 for the case where γ is relatively small compared to d and a.

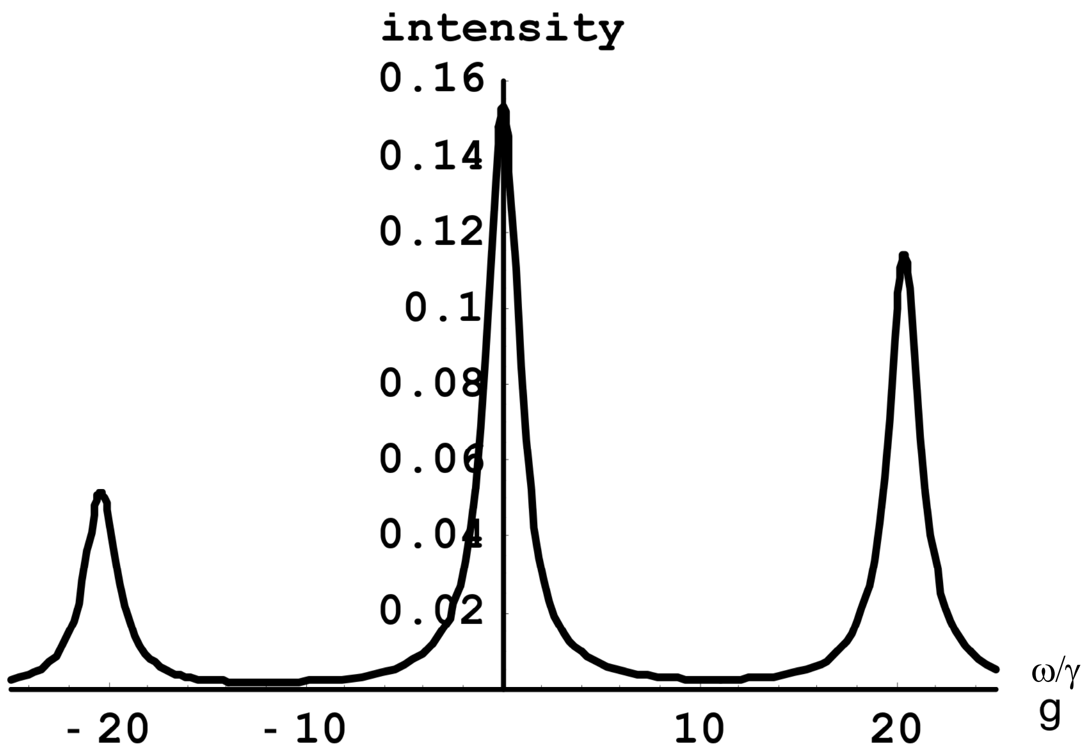

Figure 2: Normalized profile of just one σ-component (originating from the state of the parabolic quantum numbers $n_1 = 0$, $n_2 = 0$, $m = 1$) of the Ly_α line for the case of $d/\gamma = 4$, $a/\gamma = 10$, where d and a are defined in eqs. (17) and (2). The abscissa is in units ω/γ, where ω is the distance (in the frequency scale) from the unperturbed position of the spectral line and $\gamma = \gamma_p$ is the "width" due to a relatively strong Langmuir turbulence (more details are in the paragraph after eq. (18)). The profile of the σ-component originating from the state of $n_1 = 0$, $n_2 = 0$, $m = -1$ can be obtained by reflecting the above profile with respect to the ordinate axis.

Thus, the role of the allowance for the spiraling trajectories of perturbing electrons in the shift of the σ-components (compared to the standard calculations using rectilinear trajectories) is controlled by the ratio $2a/d$. Let us take as an example parameters relevant to the edge plasmas of tokamaks: $B = 5$ Tesla, $N_e = 2 \times 10^{14}$ cm^{-3}, $T_e = 8$ eV. In this situation, the ratio is $2a/d = 0.52$, so that the allowance for the spiraling trajectories of perturbing electrons is really important.

Fig. 3 shows the same as Fig. 2, but for a larger value of γ (relative to the values of d and a). It is seen that the red peak practically disappeared.

When $d/\gamma > 1$, but $a/\gamma < 1$, the unshifted subcomponent disappears: each of the two σ-components looks like a shifted singlet. This is illustrated in Fig. 4.

If $\gamma > (d^2 + 4a^2)^{1/2}$, both the blue- and red-subcomponents of a particular σ-component collapse to the position practically coinciding with the unperturbed position of the spectral line, as illustrated in Fig. 5. The entire spectral line, including the π- and σ-components, would look like a singlet structure.

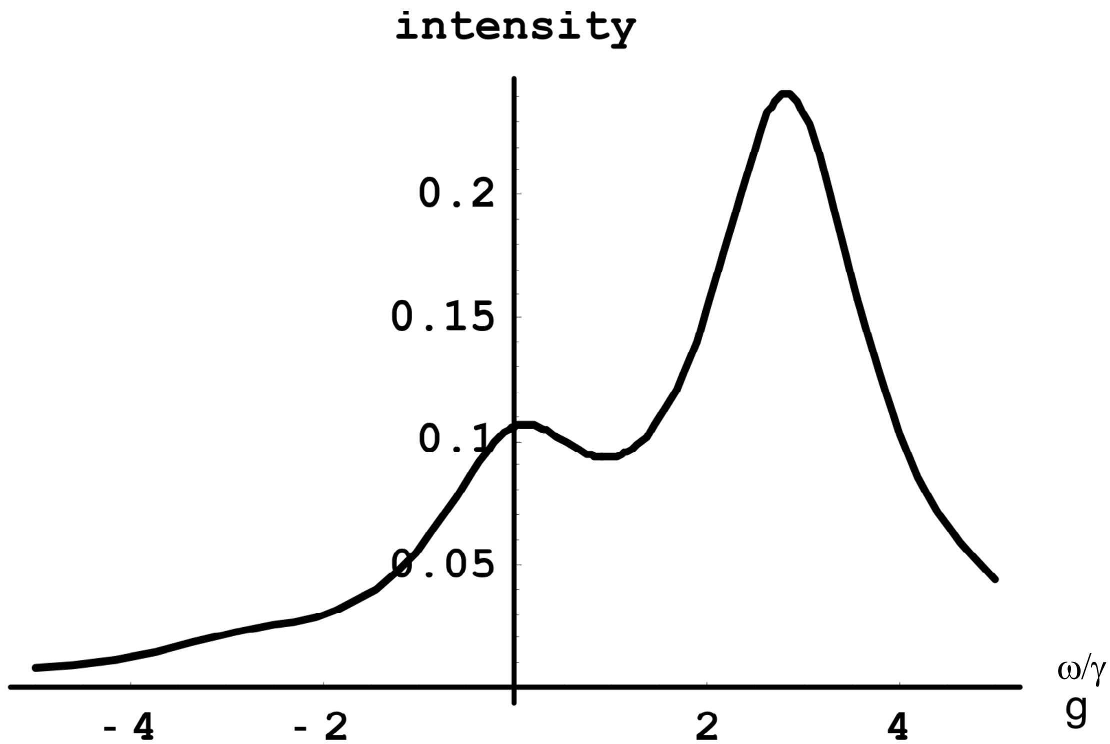

Figure 3: Same as in Fig. 2, but for $d/\gamma = 2$, $a/\gamma = 1$.

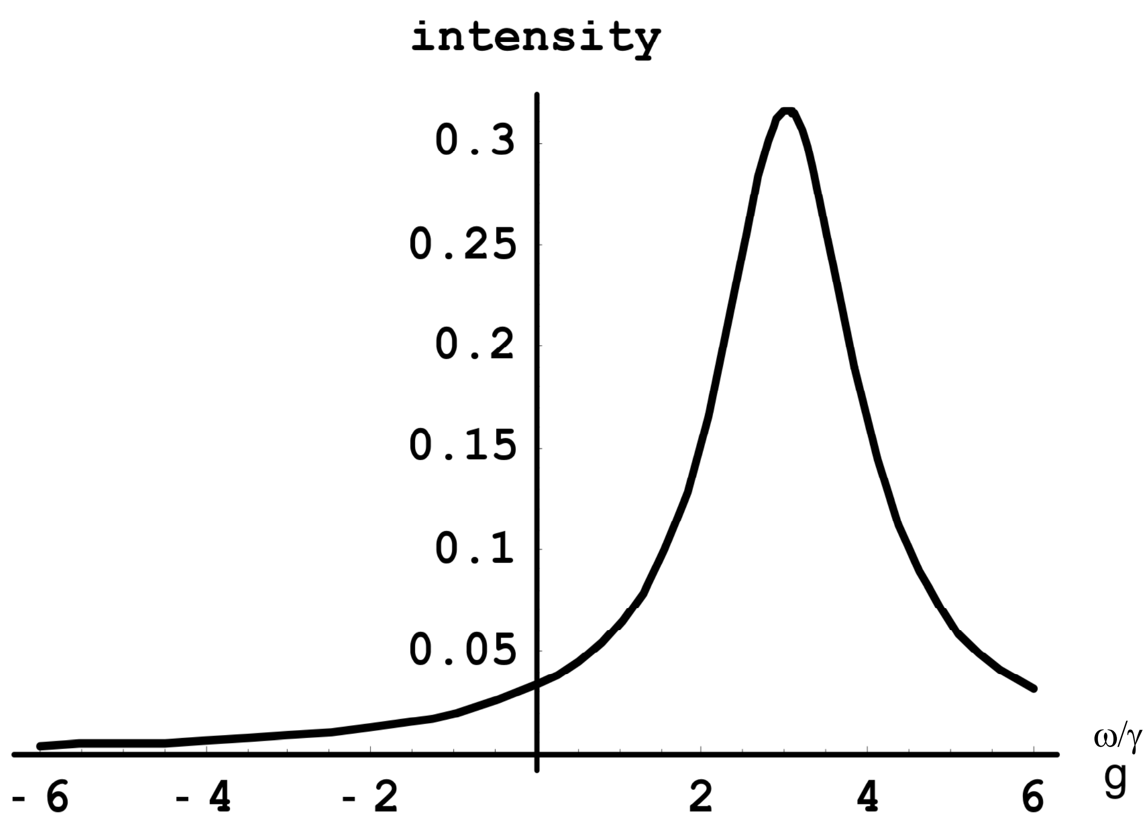

Figure 4: Same as in Fig. 2, but for $d/\gamma = 3$, $a/\gamma = 0.2$.

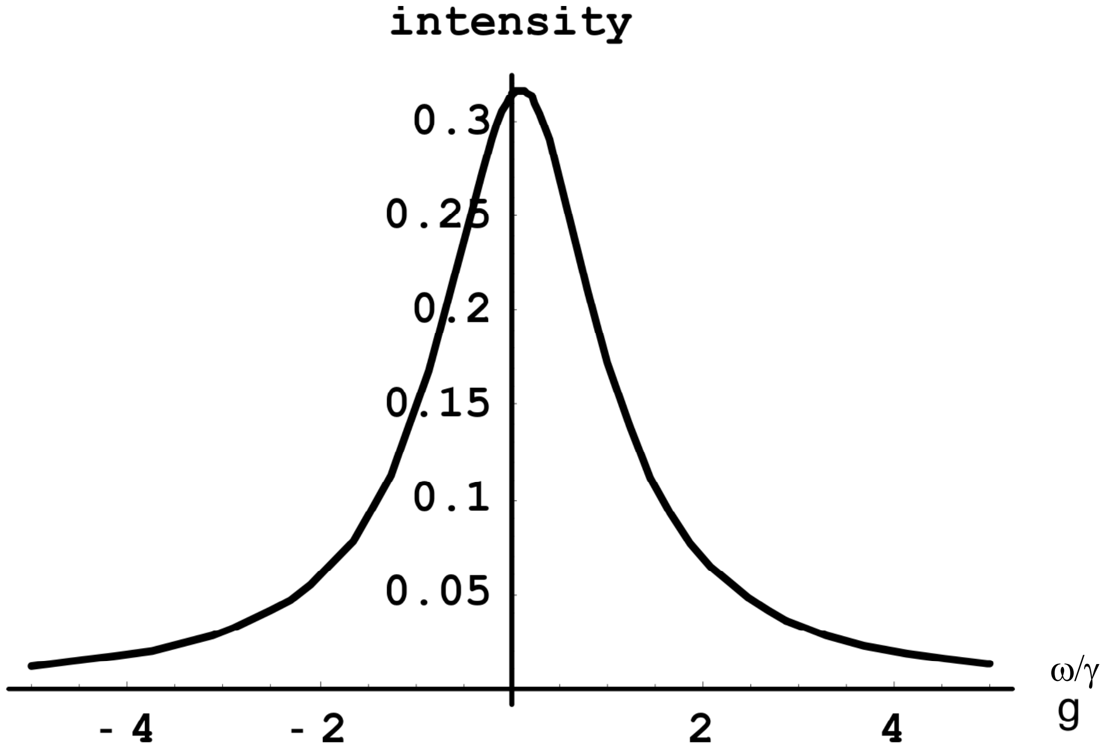

Figure 5: Same as in Fig. 2, but for *d*/γ = 0.1, *a*/γ = 0.05.

3.3. The second situation allowing to present the effect of the nonzero $\Phi^{(1)}$ in the purest form, is where the real part of the diagonal elements of the operator G is controlled by the ion dynamical broadening. In practice this relates, *e.g.*, to the lower end of the electron density range at the edge plasmas of tokamaks. For the corresponding matrix elements we can basically use the results from paper [11] obtained for the Ly_α broadening by electrons, "translate" them into the Ly_α broadening by ions, and superimpose these matrix elements with the matrix G from eq. (19) setting $\gamma_p = 0$. As a result, the total matrix, denoted as G_1, can be represented as follows:

$$G_1 = \begin{vmatrix} i(\omega - d) + \gamma & ia & 0 & ia \\ ia & i\omega + 2\gamma & ia & \gamma \\ 0 & ia & i(\omega + d) + \gamma & ia \\ ia & \gamma & ia & i\omega + 2\gamma \end{vmatrix} \tag{23}$$

Here

$$\gamma = 9g_2 \tag{24}$$

where the quantities g_n were defined by eq. (1.6) from paper [11]. The approximate value of g_2 is

$$g_2 \sim 2(\mu/T_i)^{1/2} N_i (\hbar/m_e)^{1/2} \tag{25}$$

where μ is the reduced mass of the pair "radiator – perturbing ion". We note in passing that in the matrix (23) we corrected the sign of the elements $(G_1)_{24}$ and $(G_1)_{42}$ compared to paper [11].

After inverting the matrix G_1 we obtain the following normalized profiles for each component of the Ly_α line. For the π-component:

$$I(\omega) = (\gamma/\pi)/(\gamma^2 + \omega^2) \quad (26)$$

For the σ-component originating from state (001):

$$I(\omega) = (\gamma/\pi)\{\omega^4 + 2d\omega^3 + (2a^2 + d^2 + 10\gamma^2)\omega^2 + 2d(4a^2 + 9\gamma^2)\omega + 8a^4 + 6a^2d^2 + 18a^2\gamma^2 + 9d^2\gamma^2 + 9\gamma^4\}/\{\gamma^2(5\omega^2 - 4a^2 - 3d^2 - 3\gamma^2)^2 + \omega^2(\omega^2 - 4a^2 - d^2 - 7\gamma^2)^2\} \quad (27)$$

For the σ-component originating from state (00–1), the normalized profile can be obtained from eq. (27) by changing d to $-d$.

It is seen again that, while the profile of the π-component remains unaffected by the allowance for the spiraling trajectories of perturbing electrons, the profiles of the σ-components are significantly affected by the allowance for the spiraling trajectories of perturbing electrons – both qualitatively and quantitatively.

There are qualitatively different results depending on the interplay of the two dimensionless parameters d/γ and a/γ, as illustrated in Figs. 6 – 8. When $d/\gamma > 1$ and $a/\gamma > 1$, *each* of the two σ-components looks like a triplet, as illustrated in Fig. 6.

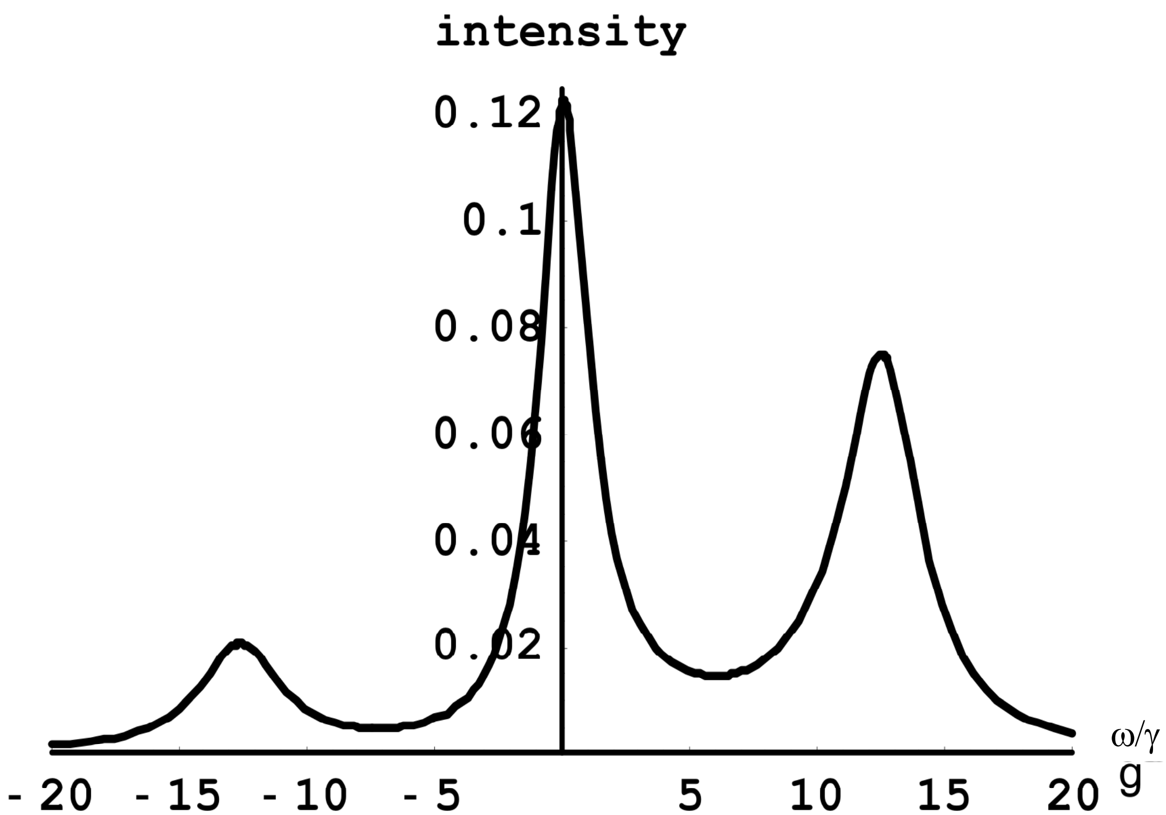

Figure 6: Normalized profile of just one σ-component (originating from the state of the parabolic quantum numbers $n_1 = 0$, $n_2 = 0$, $m = 1$) of the $Ly_{á}$ line for the case of $d/\gamma = 4$, $a/\gamma = 6$, where d and a are defined in eqs. (17) and (2). The abscissa is in units ω/γ, where ω is the distance (in the frequency scale) from the unperturbed position of the spectral line. Here γ, defined in eqs. (24), (25), is the ion dynamical "width". The profile of the σ-component originating from the state of $n_1 = 0$, $n_2 = 0$, $m = -1$ can be obtained by reflecting the above profile with respect to the ordinate axis.

When $d/\gamma > 1$, but $a/\gamma < 1$, each of the two σ-components looks like a shifted singlet. This is illustrated in Fig. 7.

Finally, when $d/\gamma \ll 1$ and $a/\gamma \ll 1$, each of the two σ-components looks like a practically unshifted singlet. This is illustrated in Fig. 8.

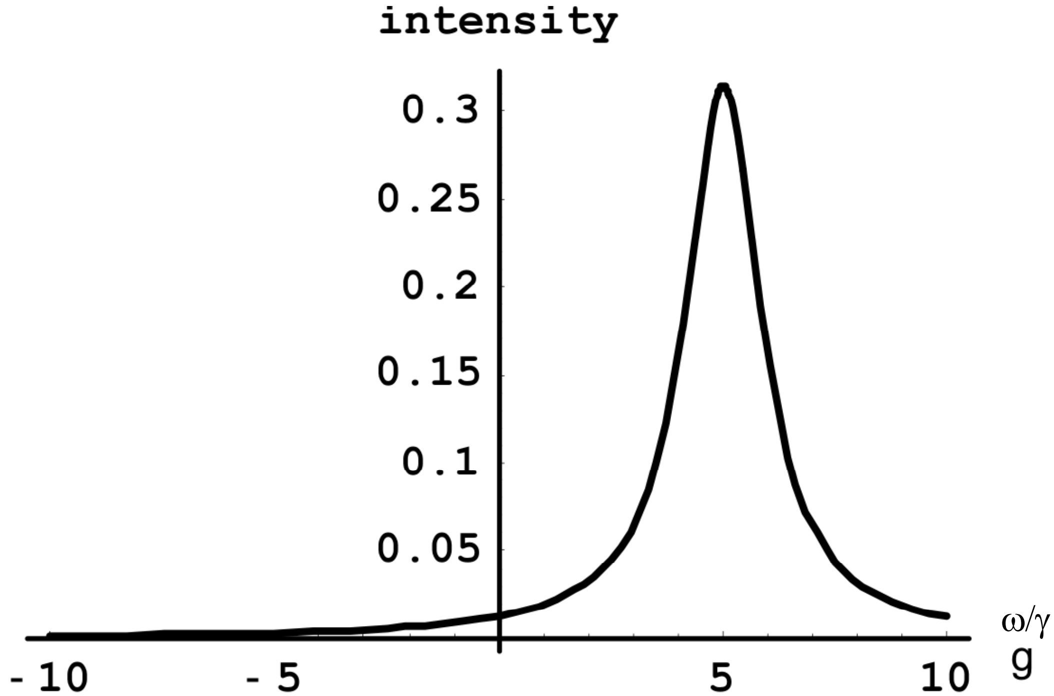

Figure 7: Same as in Fig. 6, but for *d*/γ = 5, *a*/γ = 0.25.

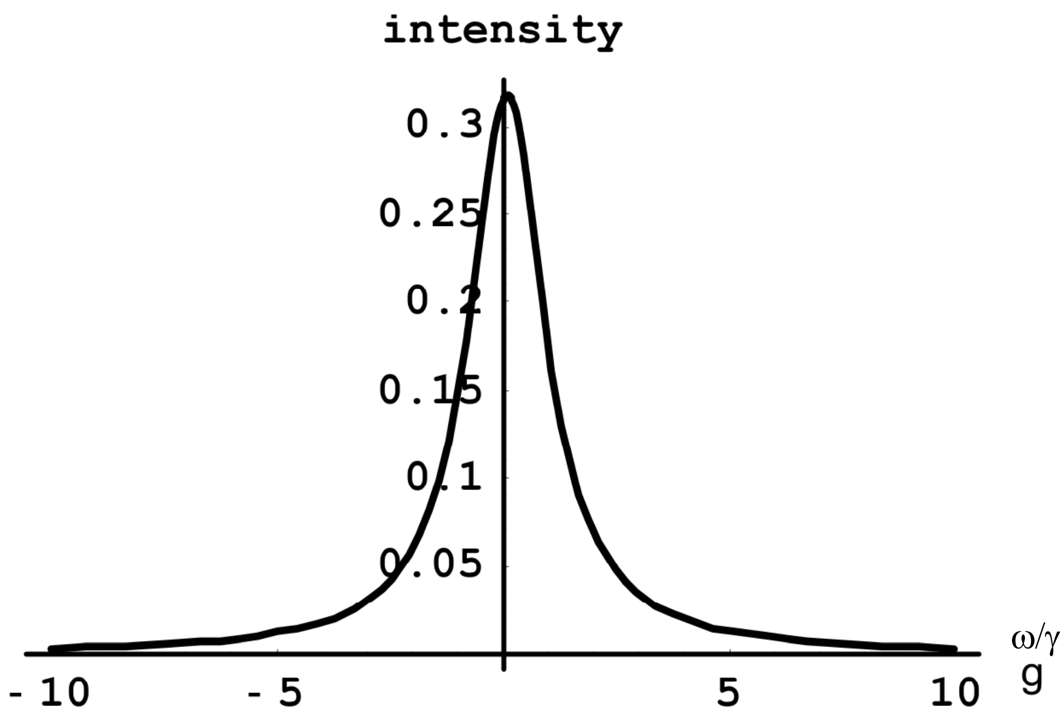

Figure 8: Same as in Fig. 6, but for d/ã = 0.1, a/ã = 0.05.

4. CONCLUSIONS

We developed the general framework for calculating shapes of hydrogen (or deuterium) spectral lines in strongly-magnetized plasmas allowing for spiraling trajectories of perturbing electrons. We showed that in this situation the first order term $\Phi^{(1)}(B)$ of the Dyson expansion of the electron broadening operator does not vanish – in distinction to the case of rectilinear trajectories, where the first non-vanishing term appeared only in the second order.

We used as an example the Ly_α line to illustrate the effects of the spiraling trajectories. We showed that the shape of each of the two σ-components can become a doublet: in addition to the shifted component, there can appear also an unshifted component. Moreover, the shape of each of the two σ-components can also become a triplet: in addition to the shifted and unshifted component, there can appear also a component shifted to the opposite wing of the line. Both the positions and the intensities of the shifted components depend strongly on the magnitude of $\Phi^{(1)}(B)$.

We focused at the effect of the non-vanishing first order $\Phi^{(1)}(B)$ of the electron broadening operator on the lineshapes – since this was the primary distinction from the case of the rectilinear trajectories. Therefore we did not calculate the effect of the spiraling trajectories on the second order $\Phi^{(1)}(B)$ – this can be done later on, if necessary.

In order to get the message across, we limited the scope of the present paper to the case of neutral radiators and limited the specific lineshapes calculations to the Ly_α line of hydrogen (or deuterium). Calculations of lineshapes of other spectral lines of hydrogen (or deuterium), as well as the general framework and the lineshapes for the case of the charged radiators, will be presented elsewhere.

References

[1] H.R. Griem, *Spectral Line Broadening by Plasmas*, (Acad. Press, New York) 1974.

[2] E. Oks, *Stark Broadening of Hydrogen and Hydrogenlike Spectral Lines in Plasmas: The Physical Insight*, (Alpha Science International, Oxford) 2006.

[3] B.L. Welch et al, Phys. Plasmas **2** (1995) 4246.

[4] U. Wagner et al, Phys. Rev. E **70** (2004) 026401.

[5] S. Fujioka et al, Scientific Reports **3** (2013) 1170.

[6] E. Oks, Sov. Phys. Doklady **29** (1984) 224.

[7] E. Oks, *Plasma Spectroscopy: The Influence of Microwave and Laser Fields*, Springer Series on Atoms and Plasmas, vol. 9 (Springer, Berlin, New York) 1995, Sect. 5.4.

[8] E. Oks, J. Phys. B: At. Mol. Opt. Phys., Fast Track Communication **44** (2011) 101004.

[9] E. Oks, in "*Atomic Processes in Basic and Applied Physics*", 2012, Springer Series on Atomic, Optical and Plasma Physics, vol. 68 (Springer, New York) p. 393.

[10] H. Pfennig, Z. Naturforsch. **26a** (1971) 1071.

[11] M.L. Strekalov and A. I. Burshtein, Sov. Phys. JETP **34** (1972) 53.